The Astrophysical Journal, 663:948–959, 2007 July 10

THE OBSERVED PROPERTIES OF DARK MATTER ON SMALL SPATIAL SCALES

Gerard Gilmore,[1] Mark I. Wilkinson,[1,2] Rosemary F. G. Wyse,[3] Jan T. Kleyna,[4] Andreas Koch,[5,6] N. Wyn Evans,[1] and Eva K. Grebel[6,7]

Received 2006 December 21; accepted 2007 March 5

ABSTRACT

We present a synthesis of recent photometric and kinematic data for several of the most dark matter dominated galaxies, the dwarf spheroidal Galactic satellites, and compare them to star clusters. There is a bimodal distribution in half-light radii, with stable star clusters always being smaller than ~30 pc, while stable galaxies are always larger than ~120 pc. We extend the previously known observational relationships and interpret them in terms of a more fundamental pair of intrinsic properties of dark matter itself: dark matter forms cored mass distributions, with a core scale length of greater than about 100 pc, and always has a maximum central mass density within a narrow range. The dark matter in dSph galaxies appears to be clustered such that there is a mean volume mass density within the stellar distribution which has the very low value of less than about 0.1 $M_\odot$ pc^{-3} (about 5 GeV/c^2 cm^{-3}). All dSph's have velocity dispersions at the edge of their light distributions equivalent to circular velocities of ~15 km s^{-1}. The maximum central dark matter density derived is model dependent but is likely to have a characteristic value (averaged over a volume of radius 10 pc) of ~0.1 $M_\odot$ pc^{-3} for the favored cored dark mass distributions (where it is similar to the mean value), or ~60 $M_\odot$ pc^{-3} (about 2 TeV/c^2 cm^{-3}) if the dark matter density distribution is cusped. Galaxies are embedded in dark matter halos with these properties; smaller systems containing dark matter are not observed. These values provide new information about the nature of the dominant form of dark matter.

Subject headings: dark matter — galaxies: dwarf — galaxies: kinematics and dynamics — Local Group — stellar dynamics

Online material: color figures

1. INTRODUCTION

The distributions of total luminosity and of central stellar velocity dispersion for star clusters and for dwarf galaxies overlap, so that the faintest galaxies have approximately the same values of these physical parameters as do star clusters, with galaxy luminosities extending as faint as ~10^3 $L_\odot$, with line-of-sight central velocity dispersions of ~10 km s^{-1}. The half-light radii (radius containing one-half the total luminosity) of the galaxies, however, are significantly larger (hundreds of parsecs) than those of star clusters (at most tens of parsecs). This leads, through the virial theorem, to significantly larger inferred masses for the dwarf galaxies, compared to star clusters of the same luminosity and velocity dispersion. Indeed, the derived values of central and global mass-to-light ratios for the gas-poor, low-luminosity, low surface brightness satellite galaxies (classified as dwarf spheroidal galaxies, dSph) of the Milky Way are high, up to several hundred in solar units, making these systems the most dark matter dominated galaxies in the local universe (see, e.g., Mateo 1998 for a convenient review of early work). As we discuss further below, they are the ideal test beds for constraining the nature of the dark matter that dominates their gravity (Ostriker & Steinhardt 2003).

The dSph galaxies and star clusters share a further observed property: organized orbital rotational energy of the member stars is negligible compared to the energy in disordered motion, which is measured by the stellar velocity dispersion at a given location. Similarly to pressure gradients in a fluid, the stellar velocity dispersion provides the support against self-gravity, but unlike the fluid case, stellar pressure can be anisotropic, generating galaxy shapes which need not be spherical. Systems in which angular momentum support against gravitational potential gradients can be ignored when analyzing the kinematics of member stars are designated as "hot."

It has been known for the past 20 years that there are well-defined, and probably fundamental, scaling relations between the half-light radius (or core radius), the central velocity dispersion, and the luminosity of hot stellar systems (e.g., Kormendy 1985; Bender et al. 1992; Zaritsky et al. 2006a, 2006b). It has further been long established that the globular star clusters in the halo of our Galaxy show distinctly different scalings from the dSph galaxies, and that the dSph galaxies in turn have different scalings from more luminous hot galaxies (e.g., Kormendy 1985, his Fig. 3; Burstein et al. 1997). Dynamical effects over their long lives have modified the size and luminosity distributions of the Galactic globular clusters (e.g., Fall & Rees 1977; Gnedin & Ostriker 1997), so it is important that robust studies include star clusters of all ages and in all environments, including globular star clusters in external galaxies, nuclear star clusters, and young massive star clusters, significantly younger than globular clusters (e.g., Walcher et al. 2005; Seth et al. 2006).

The specific combination of central velocity dispersion (σ_0) and half-light radius (r_h), $r_h^{-2}\sigma_0^{-1} \propto \rho_h \sigma_0^{-3}$, is a convenient measure of the phase-space density, where ρ_h is the mean density within

[1] Institute of Astronomy, University of Cambridge, Madingley Road, Cambridge CB3 0HA, UK; gil@ast.cam.ac.uk.
[2] Department of Physics and Astronomy, University of Leicester, University Road, Leicester LE1 7RH, UK.
[3] Department of Physics and Astronomy, Johns Hopkins University, 3900 North Charles Street, Baltimore, MD 21218.
[4] Institute for Astronomy, University of Hawaii, 2680 Woodlawn Drive, Honolulu, HI 96822.
[5] Department of Physics and Astronomy, University of California, Los Angeles, 430 Portola Plaza, Los Angeles, CA 90095-1547.
[6] Department of Physics and Astronomy, Astronomical Insitute of the University of Basel, Venusstrasse 7, CH-4102 Binningen, Switzerland.
[7] Astronomisches Rechen-Institut, Zentrum für Astronomie der Universität Heidelberg, Mönchhofstrasse 12-14, D-69120 Heidelberg, Germany.

a half-light radius. The similarity of velocity dispersion for star clusters and dwarf galaxies of the same luminosity, combined with the factor of $\sim$10 difference in their half-light radii, implies a systematic difference of some 2 orders of magnitude in the value of the phase-space density at fixed stellar mass (see, e.g., Walcher et al. 2005).

What is the physical explanation for these differences between star clusters and low-luminosity galaxies? Clearly, the presence of dark matter in dSph galaxies, but not in star clusters, is a critical distinction and provides an opportunity to identify underlying physics of dark matter (DM). For example, the suggestion by Mateo et al. (1993) that there is an apparent minimum dark halo mass of $\sim 2 \times 10^7\ M_\odot$, deduced from the available dynamical studies, implies a small-scale limit to the dark matter power spectrum unlike that assumed in ΛCDM models (e.g., Moore et al. 1999; Klypin et al. 1999). The minimum halo mass suggestion was shown to still be valid in a significantly extended sample, including dSph satellites of M31, in addition to those of the Milky Way, in an important study by Côté et al. (1999, see especially their Fig. 3). Côté et al. also provided one of the earliest robust demonstrations that the internal kinematics of dSph galaxies are in general unaffected by external tidal forces from their host galaxies, so that the results from application of equilibrium dynamical analyses are reliable. The putative minimum dark halo mass was still found to be appropriate, in the larger sample with more extensive data reviewed by Wilkinson et al. (2006) and by Gilmore et al. (2007).

Within the broad class of dwarf galaxies, of which dSph are the least luminous members, one can apply simple models to the data and obtain scaling relations between such quantities as derived central dark matter density and observed central velocity dispersion (e.g., Kormendy & Freeman 2004). The dSph galaxies are systematically discrepant in their correlation fit, falling below the extrapolated trend to larger central densities as luminosities decrease. We provide an explanation here by showing that the dSph galaxies form the limit of such relations, not a continuation. These correlations can be used to consider compatibility with various parameterizations of the power spectrum of primordial density fluctuations. Dwarf galaxies play a special role, in that they appear to be the smallest systems in which dark matter dominates, and so provide a powerful test of the power spectrum on the smallest scales. The smallest scales on which dark matter particles cluster depend on the physical characteristics of the dark matter itself (e.g., Green et al. 2005). Determining this smallest scale is the goal of the present analysis.

In this paper we revisit the established correlations and scaling relations for dwarf galaxies and for star clusters. Stellar velocity data now exist for stars across the face of several of the dSph galaxies, allowing an analysis that goes well beyond that possible with just the central value of the velocity dispersion, a limitation in early studies. The discussion below takes account of these new data, where available. Recent imaging data allow a reevaluation of the sizes of star clusters and galaxies, strengthening the case for a real discontinuity between star clusters and galaxies. We interpret our findings in terms of a more fundamental pair of intrinsic properties of dark matter itself.

2. THE SIZES AND INTERNAL KINEMATICS OF STAR CLUSTERS AND GALAXIES

The existence of a clear observational distinction between massive star clusters and low-mass galaxies has been substantially strengthened recently, both through detailed studies of more luminous and massive star clusters in a wide range of environments and through discovery of a large number of extremely low luminosity satellite galaxies around the Milky Way (e.g., Willman et al. 2005b; Belokurov et al. 2007; Zucker et al. 2006a, 2006b) and around M31 (e.g., Zucker et al. 2004, 2006c), mostly based on imaging from the Sloan Digital Sky Survey (SDSS). Figure 1 shows the current sample in a plot of half-light radius against absolute magnitude in the V band. Star clusters in all studied environments, with luminosities over the whole range from $M_V = -4$, $L \sim 10^3\ L_\odot$, up to $M_V = -15$, $L \sim 10^9\ L_\odot$, and a wide range of ages, invariably have characteristic scale sizes r_h less than about 30 pc. Thus, the dynamical range over which both star clusters and galaxies exist, and over which there is a distinct size dichotomy, has now been established to cover some 6 orders of magnitude in stellar luminosity. Available direct studies of the stellar initial mass function in star clusters and dSph galaxies (e.g., Wyse et al. 2002) show this range in luminosity corresponds to a similar dynamic range in baryonic mass. The best available data for the properties of the Galactic dwarf spheroidal galaxies are presented in Table 1.

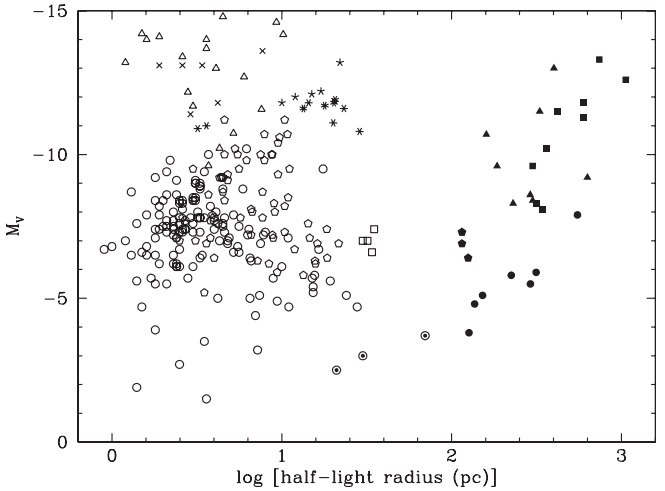

FIG. 1.—Absolute magnitude M_V vs. (logarithmic) half-light radius for well-studied stellar systems. The filled symbols show objects classed as galaxies, and the open symbols and asterisks show objects classed as star clusters of various types. Open and filled circles and filled triangles indicate objects associated with the Milky Way; open and filled squares and filled pentagons indicate objects associated with M31; and open pentagons, open triangles, asterisks, and crosses indicate more distant objects. Filled triangles show the well-known dSph galaxies, and filled circles show those recently discovered, in each case adopting the photometry listed in Table 1 (references are given in the notes). The least luminous M31 dSph galaxies (*filled pentagons*) are from Martin et al. (2006) and have $\sim$50% uncertainties. Ringed circles highlight the probable star clusters Segue 1 and Willman 1 and the object Coma Berenices. Open circles show Milky Way globular clusters, from the compilation of Harris (1996), except the two largest Galactic globular clusters (Pal 5 and Pal 14), which use the most recent data from Hilker (2006). The largest globular clusters in M31 are shown as open squares, with data from Mackey et al. (2006). Open pentagons show globular clusters in NGC 5128 (the peculiar elliptical galaxy Cen A; Harris et al. 2002, 2006; Gómez et al. 2006). Crosses represent nuclear star clusters in a range of external galaxies (Bastian et al. 2006), and open triangles represent young massive star clusters (Bastian et al. 2006; Seth et al. 2006). Asterisks show ultracompact dwarfs (UCDs) in the Fornax Cluster (De Propris et al. 2005; Mieske et al. 2002; Drinkwater et al. 2003) and in the Virgo Cluster (Haşegan et al. 2005). For UCD3* in Fornax we adopt the most recent core measurement (22 pc) by Drinkwater et al. (2003). Not shown individually are the "faint fluffy" star clusters found in the disks of lenticular galaxies (Brodie & Larsen 2002), which have absolute magnitudes $M_V \sim -7$ and sizes in the range 10–20 pc (1.0–1.3 in $\log r_h$). Sagittarius is not shown. Half-light size definitions and determinations are discussed further in the text. [*See the electronic edition of the Journal for a color version of this figure.*]

Figure 1 makes evident that there is a robust maximum radius to star clusters, at all luminosities. Figure 1 also illustrates that the dSph galaxies in both the Milky Way and in M31 have a minimum characteristic radius and that this minimum is a factor of $\gtrsim 4$ larger

TABLE 1
Observed Properties of the Established Milky Way dSph Satellites and Candidates

Object Name	L_{tot} ($L_{\odot,V}$)	Galactocentric Distance (kpc)	Half-Light Radius (pc)	Reference
Sagittarius[a]	$\gtrsim 2 \times 10^7$	24	$\gtrsim$500	...
Fornax	1.5×10^7	140	400 (core)	1
Leo I	4.8×10^6	240	330	2
Sculptor	2.2×10^6	80	160 (core)	3
Leo II	7×10^5	230	185	4
Sextans	5.0×10^5	85	630	5
Carina	4.3×10^5	100	290	6
Ursa Minor	3.0×10^5	65	300 (core)	7
Draco	2.6×10^5	80	230	8
CVn I	$\gtrsim 1 \times 10^5$	220	550	9
Hercules	$\gtrsim 2 \times 10^4$	140	310	10
Bootes	$\gtrsim 2 \times 10^4$	60	230	11
Leo IV	$\gtrsim 1 \times 10^4$	160	150	10
UMa I	$\gtrsim 1 \times 10^4$	100	290	12
CVn II	$\gtrsim 7 \times 10^3$	150	135	10
UMa II[a]	$\gtrsim 3 \times 10^3$	30	$\sim$125	13
Coma Berenices	$\gtrsim 2 \times 10^3$	45	70	10
Segue I[b]	$\sim 10^3$	25	30	10
Willman I[b]	$\sim 10^3$	40	20	14

Notes.—Quoted half-light radii are derived from Plummer model fits from the identified source, except for those cases identified as core radii. Core radii, from King model fits, are lower limits on the half-light radius.

[a] Sagittarius certainly and UMa II probably, the objects closest to the Galactic center, are associated with extended tidal streams (Belokurov et al. 2006a; Fellhauer et al. 2007). The quoted parameters in both cases are highly uncertain.

[b] Nature uncertain: suspected to be a globular star cluster.

References.—(1) Walker et al. 2006; (2) Koch et al. 2007b; (3) Mateo 1998; Westfall et al. 2006; (4) Coleman et al. 2007; (5) Kleyna et al. 2004; (6) Wilkinson et al. 2006; (7) Irwin & Hatzidimitriou 1995; (8) Wilkinson et al. 2004; (9) Zucker et al. 2006a; Ibata et al. 2006; (10) Belokurov et al. 2007; (11) Belokurov et al. 2006b; Muñoz et al. 2006a; (12) Willman et al. 2005a; Kleyna et al. 2005; (13) Zucker et al. 2006b; Grillmair 2006; (14) Willman et al. 2005b.

than the largest star clusters. With the exception of the recently discovered object Coma Berenices (Belokurov et al. 2007)—the largest and brightest of the three systems indicated by ringed circles in Figure 1, which manifestly merits further study but is one of the two new dSph galaxies that lie between the Sagittarius dwarf and the Magellanic Clouds and that show significant indications of tidal disruption—there is no known object in the size gap between $\sim$30 and $\sim$120 pc.

It is more correct to say that, modulo Coma Berenices, there is no known stable object in the size gap. This intermediate size might be occupied transiently by a larger object (a dwarf galaxy) in the very late stages of disruption by external (Galactic) tides, or by a small object (globular cluster) in the last stages of evaporation. In the first of these cases a low velocity dispersion compact core can be generated transiently, if outer, hotter, stars are removed by a suitable tide, while in the second case the density profile changes systematically from the small value typical of a compact star cluster to a very large value, almost constant density, covering all possible radii during that (short lived) process.

Willman 1 (radius 20 pc; Willman et al. 2006) and Segue 1 (radius 30 pc; Belokurov et al. 2007) are also newly discovered and interesting tests of the conclusions of this section, with Segue 1 showing evidence for significant tidal disruption. The two largest Galactic globular clusters are Pal 14, with size 28 pc, and Pal 5, 24 pc, which is in an advanced stage of tidal disruption with prominent streams of stripped stars (Odenkirchen et al. 2003). The largest ultracompact dwarf galaxies (UCDs), also with size 25 pc, are associated with the center of the Virgo Cluster and the galaxy M87, and were for a long time suspected (Drinkwater et al. 2003; Haşegan et al. 2005) of being small galaxies severely affected by tides. Our interpretation of their status, based on their position in Figure 1, is that they are simply very massive star clusters, with no associated dark matter.

There are two very recent detailed dynamical analyses of the masses of ultracompact dwarf galaxies, by Hilker et al. (2007) and by Evstigneeva et al. (2007). Hilker et al. (2007) derived dynamical masses for five ultracompact dwarfs and one dE nucleus in Fornax, while Evstigneeva et al. (2007) studied six Virgo UCDs and five very luminous Fornax UCDs. They show that all these systems are similar, in structure and dynamics, and that the dynamical mass-to-light ratios for the UCDs are consistent with simple stellar models: there is no evidence for any dark matter associated with these stellar clusters. They are the (very) high-mass/high-luminosity extreme of more typical globular cluster populations.

There are systematic effects that need to be taken into consideration when interpreting Figure 1. First, the half-light radius (whose definition is the obvious one, the radius enclosing one-half the total luminosity) can be robustly estimated only in systems with a well-defined and convergent luminosity profile. In many cases the parameter published is a "core radius," the radius at which the projected surface brightness has fallen to one-half its central value. For the commonly used King model fits to star clusters, the core and half-light radii are similar, except in (low concentration) cases where the object has an extended tail to the brightness distribution. In this case, the derived core radius underestimates the true half-light radius. For a modeled projected surface brightness $\mu(r)$ described by

$$\mu(r) = \mu_0 \left(1 + \frac{r^2}{a^2}\right)^{-\gamma/2}, \qquad (2.1)$$

where a is the scale length of the core, μ_0 the central surface density, and γ the power-law decline of the surface density at large radii, King models have $\gamma \sim 2$, and the Plummer sphere has $\gamma = 4$. The projected integrated luminosity L_p is

$$L_p(r) = \frac{2\pi\mu_0}{\gamma - 2}\left[a^2 - a^\gamma\left(a^2 + r^2\right)^{-(\gamma-2)/2}\right], \qquad (2.2)$$

where the integral to infinity is

$$L_{\rm tot} = \frac{2\pi\mu_0 a^2}{\gamma - 2}. \qquad (2.3)$$

For the Plummer sphere $L_p(a) = 1/2L_{\rm tot}$. That is, the physical meaning of the scale parameter a in this Plummer case is a half-light radius. More generally, the relation between the scale parameter a and the core radius r_c, defined as above, can be shown to be

$$r_c = a(2^{2/\gamma} - 1)^{1/2}, \qquad (2.4)$$

where a is the (cylindrical) radius which encloses one-half the total luminosity, so that for a Plummer sphere observed in projection the half-light radius a and core radius r_c are related by $a \approx 3r_c/2$. Core radii, where fitted, are adequate approximations to half-light radii for King model globular star clusters and are lower limits to half-light radii for dSph galaxies, while the Plummer scale parameter is a half-light radius, to the accuracy of a Plummer model fit to the data. Conservatively, we adopt and identify three cases of core radii for dSph galaxies at face value, rather than converting to larger, but more uncertain, half-light radii.

Second, only the extent of the baryonic component is being measured, and there is no guarantee—or need—for mass to follow light. Given that most, if not all (as we argue here), galaxies are embedded in extended dark matter halos, photometric determinations are probably a lower limit on the scale length of the total mass distribution (we discuss this below for two specific cases, Ursa Minor and Fornax). Figure 1 is therefore probably conservative in describing mass: an even larger distinction between star clusters and dSph galaxies would be seen were one able to plot parameters describing mass rather than light.

Figure 1 is further conservative in that it is possible that the recently discovered very low luminosity dSph galaxies are in fact larger than is shown. The recent history of observational studies of nearby low-luminosity galaxies, in which individual stars are resolved and the extent on the sky is measured through star counts, corrected for foreground stars in the Milky Way, has been that their radial extents (and hence total luminosities and half-light radii) tend to be somewhat underestimated (e.g., Odenkirchen et al. 2001). As photometric data are extended to lower surface brightnesses, and as kinematic studies of individual member stars develop, allowing foreground stars to be rejected on the basis of line-of-sight velocity, the galaxies are typically found to be larger than first measured. For example, for the best-studied dSph the estimated total extent has changed by a factor of 1.5–2 over the last 10 years. In contrast, star clusters really do have steep outer light profiles and thus have well-defined observational parameters. Both these effects lead to a systematic observational underestimate of any gap in spatial scale between star clusters and galaxies.

3. MASSES AND MASS DISTRIBUTIONS, CORES AND CUSPS

It has long been known that the observed value of $\sim$10 km s^{-1} for the line-of-sight velocity dispersions of Local Group dwarf spheroidals (dSph's), together with their $\sim$200 pc half-light radii, implies mass-to-light ratios M/L of up to $\gtrsim 100\ M_\odot/L_\odot$. Until recently, most of these estimates of M/L were based on a measurement of only the central value of the velocity dispersion and on the assumption that the mass profile follows the light profile. The availability of data sets of radial velocities for hundreds of individual stars spread out in radius across the nearby dSph's, obtained by several groups, has changed all this. To date, the line-of-sight velocity dispersion profiles in the Fornax, Draco, Ursa Minor (UMi), Carina, Leo I, Leo II, Sextans, and Sculptor dSph's have been mapped to the (rather poorly defined concept of an) optical edge (Mateo 1997; Kleyna et al. 2002; Wilkinson et al. 2004, 2006; Muñoz et al. 2005; Sohn et al. 2007; Koch et al. 2007b; Battaglia et al. 2006; Walker et al. 2006)—see Figure 2 for a sample of profiles obtained by our group. Central velocity dispersions have been derived for several of the newly discovered extremely low luminosity dSph satellites of both the Milky Way and M31 (Kleyna et al. 2005; Ibata et al. 2006; Muñoz et al. 2006a). Several major studies are underway so that all the known dSph galaxy satellites with $-13 \lesssim M_V \lesssim -8$ will soon have much improved determinations of their dynamical mass distributions inside their optical radii, while some information will be available on the several dSph galaxies with $-8 \lesssim M_V \lesssim -4$. Our conclusions in this paper lead us to predict extended dark matter halos for the systems with characteristic radii that place them in the "galaxy" regime of Figure 1. Future more extensive studies of these very faint galaxies, as well as continuing discoveries, will allow our predictions to be tested.

3.1. *Mass Modeling for Hot Stellar Systems*

Stellar systems with no net internal angular momentum maintain their scale size by the pressure support of random stellar motions against the gravitational potential gradient. This pressure is naturally triaxial in a collisionless system. A robust dynamical analysis of such a system involves solution of the collisionless Boltzmann equation (CBE) for some appropriate (stellar) tracer particle phase-space distribution function, determining the mass distribution which generates the gravitational potential gradients along which the stars orbit. Such models are being applied and further developed (Kleyna et al. 2001; Wilkinson et al. 2002; Walker et al. 2006) to the few best-studied dSph galaxies. Such analyses are appropriate for, and require, velocity and position data for (at least) several hundred tracer stars distributed across the dSph. For most dSph galaxies studied to date, the more limited data available justify analysis only of the first velocity moment of the distribution function, the velocity dispersion as a function of radius.

In a collisionless equilibrium system the Jeans equations are the relation between the kinematics of the tracer stellar population and the underlying (stellar plus dark) mass distribution. In terms of the intrinsic quantities, and assuming spherical symmetry, the mass profile can be derived as

$$M(r) = -\frac{r^2}{G}\left(\frac{1}{\nu}\frac{d\nu\,\sigma_r^2}{dr} + 2\frac{\beta\sigma_r^2}{r}\right), \qquad (3.1)$$

where $\sigma_r(r)$ is the one-dimensional (1D) stellar velocity dispersion component radially toward the center of the mass distribution, $\beta(r)$ quantifies the stress term associated with (possibly radially variable) velocity orbital anisotropy, and $\nu(r)$ is the stellar density distribution.

The quantities directly observed are the line-of-sight velocity dispersion as a function of projected radius, R, $\sigma_{-p}(R) = \langle v(R)^2\rangle^{1/2}$

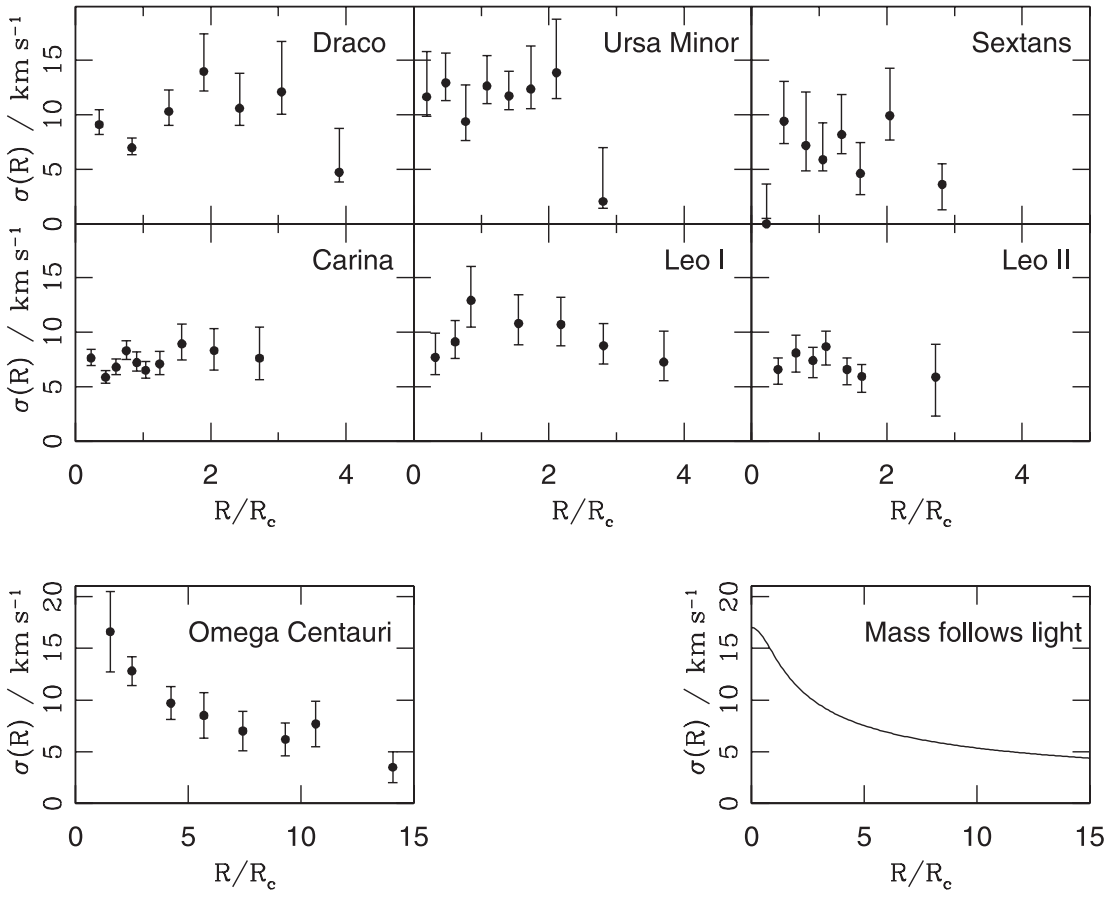

FIG. 2.—Observed line-of-sight velocity dispersion profiles for six dSph galaxies. Also shown (*bottom right*) is the model-predicted dispersion profile for a Plummer model in which mass follows light. The bottom left panel shows the observed velocity dispersion profile for the globular cluster ω Cen from Seitzer (1983). The similarity between the Plummer mass-follows-light model and the data for ω Cen is apparent, with a monotonic decrease in dispersion from a central maximum. In contrast, the dSph galaxies do not have their maximum dispersion value at the center and retain relatively high dispersions at large radii, indicating extended (dark) mass distributions.

and the surface brightness profile as a function of projected radius. Given finite amounts of data defining the projected surface brightness and kinematic distribution functions, we can proceed in either of two ways. We can assume a priori a parameterized mass model $M(r)$ and velocity anisotropy $\beta(r)$ and fit the observed velocity dispersion profile, or we can use the Jeans equations to determine the mass profile from the projected velocity dispersion profile, utilizing some (differentiable) functional fit to the observed light distribution and a (range of) assumed form(s) for the anisotropy $\beta(r)$. Assuming spherical symmetry, it is straightforward to obtain $\langle\sigma_r^2\rangle$ from the observed line-of-sight velocity dispersion using Abel integrals. In what follows, we take the second approach to the Jeans equation analysis: both the spatially binned dispersion profile and the surface brightness distribution are fit by an appropriate smooth function, and we assume an isotropic velocity dispersion. Figure 3 shows some examples of the fits to the light and dispersion profiles used in the analysis.

It is obvious from the Jeans equation that radially variable velocity dispersion anisotropy is degenerate with mass, making any deductions as to whether or not the inner mass profile is cored or cusped in general model dependent. Further information is needed to break this degeneracy and fortunately is sometimes available, as we discuss below. In general, however, full multicomponent distribution function models using adequately large data sets, as discussed in § 3.4 below, are required to use the information in the data to break this degeneracy.

3.2. *Moment Equation Analyses of Inner Dark Mass Distributions*

Jeans equation dynamical analyses generate three quantities. The most robust is the *mean* dark matter mass density inside the radius where adequate kinematic data are available. Similarly robust is the total mass, again inside the radius where adequate kinematic data are available. The analysis can also constrain the

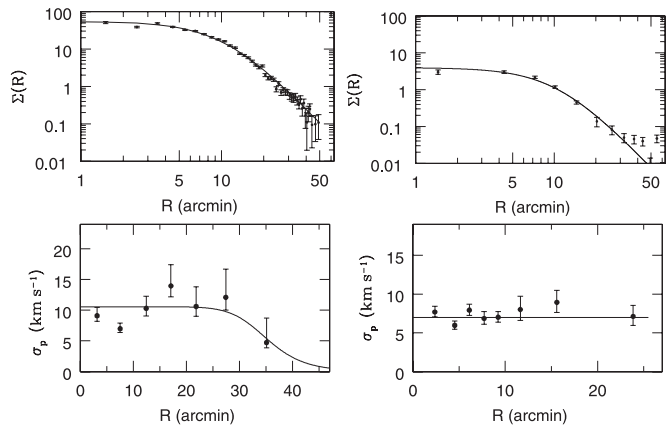

FIG. 3.—Functional fits to the surface brightness profile (*top*) and velocity dispersion profile (*bottom*) of the Draco (*left*) and Carina (*right*) dSph's used to derive mass profiles based on the Jeans equations. Similar fits are used for the remaining four dSph's presented in Fig. 4.

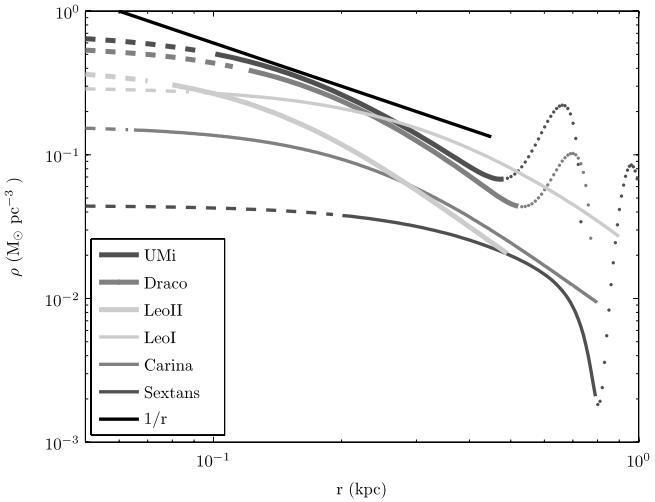

FIG. 4.—Derived inner mass distributions from isotropic Jeans equation analyses for six dSph galaxies. The modeling is reliable in each case out to radii of $\log(r)\mathrm{kpc} \sim 0.5$. The unphysical behavior at larger radii is explained in the text. The general similarity of the inner mass profiles is striking, as are their shallow profile and their similar central mass densities. Also shown is an r^{-1} density profile, predicted by many CDM numerical simulations (e.g., Navarro et al. 1997). The individual dynamical analyses are described in full as follows: UMi in Wilkinson et al. (2004), Draco in Wilkinson et al. (2004), Leo II in Koch et al. (2007a), Leo I in Koch et al. (2007b), Carina in Wilkinson et al. (2006, 2007, in preparation), and Sextans in Kleyna et al. (2004). [*See the electronic edition of the Journal for a color version of this figure*.]

mass density in a small central region, although the limited central spatial sampling makes this less robust and dependent on an adopted underlying mass density profile. It remains the case, of course, that a suitably small central cusp in the mass distribution would not be detected so long as it was unresolved inside the available kinematic data: very small cusps might be present.

Our Jeans analysis mass models are presented in Figure 4. Some caution is required in the interpretation of these profiles, given the simplifying assumptions which have been made (spherical symmetry, velocity isotropy, and smooth dispersion and light profiles). First, given that satisfying the Jeans equations is a necessary, but not sufficient, condition for a solution of the CBE to be everywhere nonnegative (and hence a viable distribution function), the models presented here are not guaranteed to correspond to physical models. However, we note that for a tracer distribution with an isotropic velocity distribution and density profile $\nu \sim r^{-\gamma}$, the logarithmic slope of any external power-law potential $\psi \sim r^{-\delta}$ must satisfy $\delta \leq 2\gamma$ to ensure the nonnegativity of the distribution function (An & Evans 2006). Thus, it is reasonable to assume that for a tracer distribution with $\gamma \sim 0$, a cored mass density distribution will yield a physically meaningful distribution function. Second, in this analysis we have assumed specific forms for the light distribution: the mass profiles obtained will be sensitive to these assumed forms. However, as Figure 3 illustrates, our profiles constitute reasonable representations of the observed data—but it is worth recalling that the very innermost light profiles of the dSph's are often poorly defined.

Our representation of the velocity dispersion profiles as smooth functions which are flat in the innermost regions may mask features which are visible in the profiles at marginal significance. It has been known for many years that the stellar populations in dSph galaxies are complex, with the implications of this complexity evident in many analyses, yet difficult to model fully without very large data sets. With respect to a superposition of two populations, one should be careful when comparing this to the observed star formation histories. Episodic star formation with clearly distinguished periods of star formation has been detected only in Carina; all other dSph's with extended star formation histories show evidence of long-lasting activity without obvious pauses. So one is not really dealing with, e.g., only two distinct populations (as is sometimes claimed in the literature). It can be shown, however, that younger and/or more metal-rich populations are more centrally concentrated (e.g., Harbeck et al. 2001) and that these populations also tend to exhibit lower velocity dispersions (Tolstoy et al. 2004). Recently, McConnachie et al. (2006) have recalled the general point that a rising dispersion profile (e.g., Leo I) might arise from the superposition of two populations in the dSph with different velocity dispersions and spatial scale lengths. While this is certainly an interesting suggestion, we note that all our assumed functional fits to the observed dispersion profiles are statistically consistent with the observed data.

Given these caveats, we conclude that the Jeans analysis demonstrates that the observed velocity dispersion profiles and cored light distributions of dSph's are likely to be consistent with their inhabiting dark matter halos with central cores. We note that there is no reason that the photometric scale length is exactly the underlying mass scale length. From the mass modeling, the lower limit on mass density core size is constrained to be at most a factor of 2 smaller than the observed luminosity core in UMi and Fornax. Similarity, rather than exact equality, of the two scales is what is relevant here. As discussed below, however, cusped mass distributions can also reproduce the observed data on the light profile and velocity dispersion profile. To determine the actual slopes of the inner dark matter density profiles, further information, either in the form of larger velocity data sets which permit full distribution function modeling (see below) or complementary dynamical evidence, is required. Fortunately, in two special cases, those of UMi and Fornax, there is additional information that enables us to distinguish between shallow and steep internal mass density profiles.

In UMi, an otherwise very simple system from an astrophysical perspective, an extremely low velocity dispersion substructure exists. Kleyna et al. (2003) explain this as a star cluster, which has become gravitationally unbound (the normal eventual fate of every star cluster) and which now survives as a memory in phase space. Why does it survive in configuration space? The group of stars has the same mean velocity as the systemic velocity of UMi, so it must orbit close to the plane of the sky, and hence through the central regions of UMi. As Kleyna et al. (2003) show, persistence of the cold structure is possible only if the tidal forces from the UMi central mass gradient are weak. In fact, survival of this phase-space structure in configuration space requires that UMi has a slowly varying inner mass profile, that is, a core, rather than a cusp.

The Fornax dSph galaxy has five surviving globular clusters. The orbit of a compact massive system, such as a globular cluster, should decay due to dynamical friction as it orbits through the background dark matter halo particles. The rate of this orbital decay is faster in a steep (cusped) dark matter density profile and is slower in a shallow (core) dark matter density profile. The (projected) distribution of the surviving clusters has been analyzed most recently by Goerdt et al. (2006), who show that a cored mass distribution is strongly preferred.

In summary, while Jeans equation dynamical analyses cannot be assumption independent, in both cases where some independent information is available, shallow (cored) mass distributions are preferred. There is no case where a steep (cusp) distribution is

TABLE 2
Dynamical Relaxation Times for dSph and Star Cluster Densities

Number of Stars	Radial Scale (pc)	1D Velocity Dispersion (km s^{-1})	Crossing Time (yr)	Relaxation Time (yr)	Dynamical Age	Object Type
100	2	0.5	4×10^6	10^7	$\gtrsim 1$	Open cluster
10^5	4	10	4×10^5	4×10^8	$\gtrsim 10$	Median globular cluster
10^8	10	30	3×10^4	2×10^{10}	~ 1	Nuclear/large globular cluster
10^{12}	10^4	300	3×10^7	10^{17}	10^{-7}	gE galaxy
10^9	10^3	50	2×10^7	10^{14}	10^{-4}	dE galaxy
10^8	400	10	4×10^7	10^{13}	10^{-3}	dSph galaxy

required by the data. Applying Occam's razor, we therefore assume for the remainder of this analysis that all dSph galaxies have similar underlying dark matter mass profiles, which are cored. We adopt this specific case-dependent result as a general result since it provides a natural context for a characteristic length scale, which is suggested by Figure 1. A single mass model, supported in two specific cases with suitable data, links two otherwise disparate results, one photometric, one kinematic.

3.3. *King Model Dynamical Analyses*

Dynamical analysis requires some simple and mathematically smooth functional description of the spatial distribution of the stellar tracers of the gravitational field. While any smooth function is adequate, those most frequently used include Plummer models and King models. Each is convenient but can mislead if the parameters in the adopted fitting function are (over)interpreted as having physical meaning.

The King model (King 1966; see also Binney & Tremaine 1987) is physically valid for a self-gravitating system with a velocity distribution function which is a lowered Maxwellian, i.e., approximates an isothermal distribution at small radii, with an imposed small core—to avoid an unphysical divergence—and an imposed cutoff at large radii—to prevent infinite extension and infinite velocities. This model is a good description of a stellar globular cluster, in which mass follows light. The equilibrium velocity distribution function which underlies this model is that generated by cumulative long-range gravitational interactions between the component stars, which brings a system of N stars with rms velocity dispersion v, scale size R, and corresponding crossing time $t_{\rm cross}$ into dynamical equilibrium in a characteristic time $\approx (N/8 \ln N) t_{\rm cross}$, where $t_{\rm cross} \approx R/v$. It is therefore naturally appropriate to any system in which the astrophysical lifetime is long compared to the dynamical relaxation time, and in which stars are orbiting in a gravitational potential generated self-consistently from their mass.

We review the relevant range of applicabilities in Table 2. Only the systems in Table 2 with dynamical age $\gtrsim 1$ are amenable to a physically meaningful King model analysis, where we define "dynamical age" as the ratio of the astrophysical age to the relaxation time. Dwarf spheroidal galaxies have a dynamical age 3–4 orders of magnitude outside this range of validity, being too young in a dynamical sense.

We may ask what would be the stellar mass of a system with the internal velocity dispersion and spatial scale size of a representative dSph galaxy, and which has its dynamical relaxation time less than the Hubble age of the universe, so that the physical conditions appropriate to establish a King model are in place. The result is that one requires a stellar system of 5×10^{10} stars. For a plausible stellar mass to light ratio, this implies a galaxy of luminosity $\gtrsim 10^{10} L_\odot$. Observed dSph galaxies are many orders of magnitude less luminous. Thus, one does not expect that a King model will be a physically valid description of a dSph galaxy, although, as Table 2 shows, one does expect such models to be reasonable approximations for massive star clusters. While it may still be convenient to use a King model as a fitting function for a galaxy, it is invalid to interpret the two free parameters of that fit—the "core radius" and the "tidal radius"—as meaningful physical properties of the galaxy. Wu (2007) also shows that King models are inadequate descriptions of available dSph kinematics.

More generally, there are unavoidable consistency requirements in any mass-follows-light model. In any model where mass follows light the projected velocity dispersion must be maximum at the center, and then fall monotonically. For a well-mixed (star cluster) system, the velocity dispersion will decrease by roughly a factor of 2 over three core radii. This is an unavoidable requirement for any mass-follows-light system and is observed in star clusters (Fig. 2). Such a velocity dispersion profile is not required by data in any well-studied galaxy, however small, further emphasizing the intrinsic difference between (virial, King) star clusters and galaxies.

3.4. *Time-dependent Kinematics and Radial Range of Valid Analysis*

Determination of the mass distribution in the outer parts of a dSph satellite galaxy remains a complex and data-starved challenge. The (very few) tracer stars at large radii occupy the extreme limits of the kinematic distribution function, where simplifying assumptions are least reliable. At some radius tidal forces from the Milky Way must become important, violating the equilibrium dynamics assumption, although that radius depends on the a priori unknown dSph dark matter distribution and the (usually poorly constrained) orbit of the dSph around the Galaxy.

Very many studies are available predicting the effects of time-dependant tides on the structure and kinematics observable in the outer parts of galaxies. However, most such studies are idealized and consider only single-component models—i.e., either no dark matter or only dark matter, as one prefers (Johnston et al. 1999, 2002; Sohn et al. 2007). This makes any comparison to observations of the stellar density distribution or of the stellar kinematics in a dSph galaxy with a dark matter halo at best problematic. One recent example, among several, which illustrates the richness of the potential tidal effects on stars orbiting in dark matter potentials is that of Read et al. (2006b), which is one of the few studies to consider external tidal effects on two-component dSph models in which stars orbit inside a dark matter halo. In another study of tides, Klessen et al. (2003) model the available data for the Draco dSph, under the assumption that there is no dark matter (i.e., a single-component model), so that the dSph is unbound. They deduce that the present smoothness and small line-of-sight depth of this galaxy make unbound models impossible, and conclude that dynamically dominant dark matter is required.

The observed kinematic and spatial distributions in the outer parts of the dSph remain poorly determined by observations. As may be seen in Figure 2, there is some evidence for low-dispersion (cold) outer populations (Wilkinson et al. 2004) and for flat velocity dispersion profiles to large distances (Sohn et al. 2007; Muñoz et al. 2005), both of which are inconsistent with simple tidal disruption effects, particularly since most dSph's show no evidence of apparent rotation (Koch et al. 2007b), another prediction of tidal disruption models (Read et al. 2006b). Carina may be an exception, as Muñoz et al. (2006b) have recently detected a velocity gradient on large scales (beyond the nominal King model fit "tidal" radius) in this dSph. Photometric studies continue to be inconclusive, with some suggesting a characteristic signature of tidal distortions (e.g., Irwin & Hatzidimitriou 1995; Sohn et al. 2007), but with later studies of the same galaxy failing to find any signal from improved data (Odenkirchen et al. 2001; Ségall et al. 2007). Considerable uncertainty about the dynamical state of the three dSph's nearest to the Galactic center, however, remains, with the closest one—Sagittarius—being manifestly disrupted.

Fortunately for our present purposes, which are concerned with the properties of the mass distribution in the inner regions of the dSph, the dynamical state of the very outer parts of the dSph is relatively unimportant. The complexities noted do mean any discussion of total masses is currently impracticable.

We also note for now that if indeed it is shown from future studies that dSph galaxies are *not* strongly dark matter dominated, but are star-cluster–like stellar systems whose structural and kinematic properties have been inflated in some way, the conclusions of this paper concerning a minimum scale length on which dark matter is seen to concentrate are inevitably and drastically strengthened. The minimum dark matter clustering scale would have to extend beyond that derived here, and become of the order of 1 kpc.

3.5. *Distribution Function Modeling*

A known limitation of Jeans equation moment analyses is that (at least) some of the dSph galaxies show complex stellar populations, so that adoption of a single dispersion profile and single length scale is necessarily a simplification. In all cases these Jeans moment analyses are applicable only over the range where simple functions provide an adequate description of the underlying galaxy, which in general is limited to one to two physical (luminous) scale lengths. More complex behavior, preventing valid application of such simple models, is seen in the very outer parts of most dSph galaxies studied to date, where also identification of member stars becomes increasingly uncertain. In general, a more robust analysis requires significantly more information.

As larger data sets become available distribution function modeling can supersede use of the Jeans moment equations. In distribution function analyses one proceeds by constructing parameterized equilibrium dynamical models, allowing the dark halo shape and mass and the tracer velocity anisotropy to vary. From these models one can determine model distributions of the observable line-of-sight velocity. These models are then convolved with observational errors and an orbital velocity distribution for binary star systems appropriate to a data set of interest, to predict observable velocity distributions at every point across the projected galaxy. It is then straightforward to determine the best-fitting models using the individual stellar velocities, without the need to degrade the data into moments (dispersions).

Models of this type have been applied by Kleyna et al. (2001) and by Walker et al. (2006) and are being developed further for future application to all large available data sets. Mass-follows-light models for Draco were ruled out at the 2.5 σ confidence level using this type of analysis (Kleyna et al. 2001). Constant anisotropy models of this type favor rather shallow halo inner mass profiles with $\rho \propto r^{-0.5}$ (Magorrian 2003; Koch et al. 2007b).

A form of distribution function modeling has recently been used by Penarrubia et al. (2007), who apply a methodology developed by Lokas (Lokas 2002; Lokas et al. 2005) to fit observed dispersion profile data adopting a King model for the luminous galaxy and embed this inside an assumed Navarro-Frenk-White (NFW) dark halo. This analysis requires, as is usual in such fitting of NFW models, very considerable dark masses associated with the observed dSph. NFW virial masses for the dwarfs considered in this paper are all larger than $10^9\,M_\odot$, with that for Draco having log (mass) $= 9.8\,M_\odot$. This form of modeling breaks the degeneracy in the mass determination discussed above essentially by requiring that the assumed dark halo be of NFW form.

Wu (2007) has recently applied more general distribution function models to a rebinned version of the data for Draco and UMi shown in our Figure 2 here (excluding our outermost data), and for other published data for the Fornax dSph. Wu's analysis considers both two- and three-integral distribution function models, assuming the galaxies are stable axisymmetric systems embedded in spherical dark matter potentials. He includes a range of forms for the underlying gravitational potential, considering constant density models, constant mass-to-light ratio models, dominant central point-mass (massive black hole) models, NFW models, power-law models, and isochrone models. Wu's isochrone model is closest in form to those derived here in our Jeans analysis (Fig. 4), having an inner cored mass profile out to some radius determined by fitting to the data, beyond which the profile of the dark matter distribution steepens.

Wu's analysis shows that all of the NFW, power-law, and isochrone models are consistent with the data, while the constant density, constant mass-to-light ratio, and dominant central black hole models are strongly ruled out. This conclusion is in very good agreement with results of our analysis in this paper, where we use additional information to prefer cored mass models (isochrone-like potentials) over the NFW and pure power-law cases. Wu's characteristic scale lengths at which the underlying dark matter density breaks below the cored inner distribution are 500, 200, and 900 pc for Draco, UMi, and Fornax, respectively. These results are quite consistent with the results of the simpler Jeans analysis we present here.

3.6. *Mass Distributions in dSph Galaxies*

There are several Jeans equation analyses of dSph kinematic data which are fully described in the recent literature. Figure 4 summarizes the results of these Jeans equation models for several of the dSph galaxies from Wilkinson et al. (2006) with more recent results for Leo I from Koch et al. (2007b) and for Leo II from Koch et al. (2007a), with in each case the simplest possible assumptions for the velocity distribution, namely, that it is isotropic at all radii. It is apparent that the models are invalid at large radii, where an unphysical oscillation in some of the mass profiles is derived. In the inner regions the models are well behaved and reproduce the overall shape of the observed dispersion and light profiles. As illustrated in detail in, for example, Koch et al. (2007b, especially their Fig. 11), for Leo I, both cored and cusped mass models can provide acceptable agreement with the data for a suitable value of a constant anisotropy, and excellent agreement when allowing a radially variable stellar orbital anisotropy. As described above, although the Jeans models alone cannot distinguish between cored and cusped mass distributions, in those two

TABLE 3
OBSERVED VELOCITY DISPERSIONS FOR MILKY WAY SATELLITES AND DERIVED MASSES AND DENSITIES

Galaxy Name (1)	σ (km s^{-1}) (2)	$r_h\sigma^2/G$ ($M_\odot$) (3)	r_{max} (kpc) (4)	M_{DM} ($M_\odot$) (5)	$\overline{\rho_{DM}}(r_{max})$ (GeV/c^2 cm^{-3}) (6)	$\overline{\rho_{DM,cusp}}$(10 pc) (GeV/$c^2$ cm^{-3}) (7)	$v_{circ}(r_{max})$ (km s^{-1}) (8)	Phase-Space Density ($M_\odot$ kpc^{-3} km s^{-3}) (9)	Reference (10)
Fornax	11.1 ± 0.6	1×10^7	1.5	$\sim 3 \times 10^8$	~0.7	1.1×10^3	29	2×10^4	1
Leo I	9.9 ± 1.5	8×10^6	$r_{lim} \sim 0.9$	$(3–8) \times 10^7$	~0.3–0.9	310–830	12–20	3×10^4	2
Sculptor	7–11	2×10^6	$r_{lim} \sim 1.8$	$\gtrsim 10^7$	~0.015	27	...	2×10^5	3
Leo II	6.8 ± 0.7	2×10^6	$r_{lim} \sim 0.5$	3×10^7	~1.8	~930	16	1×10^5	4
Sextans	8	9×10^6	0.8	$\sim 3 \times 10^7$	~0.5	390	13	9×10^3	5
Carina	7.5	4×10^6	$r_{lim} \sim 0.8$	$\sim 4 \times 10^7$	~0.7	520	15	4×10^4	6
Ursa Minor	12	1×10^7	0.5	$\gtrsim 6 \times 10^7$	~4.5	2.1×10^3	23	3×10^4	7
Draco	13	9×10^6	0.5	$\gtrsim 6 \times 10^7$	~3	1.7×10^3	22	4×10^4	7
Bootes	6.6 ± 2.3	2×10^6	...	$\sim 10^7$	...	...	...	8×10^4	8
UMa I	9.3	6×10^6	...	$\sim 10^7$	...	...	...	4×10^4	9

NOTES.—Col. (1): Galaxy name. Col. (2): Total velocity dispersion from extant data (as quoted in associated reference in col. [10]). Col. (3): Crude mass estimate based on total velocity dispersion. Col. (4): Radial extent of mass models—the radial extent quoted is either the actual region within which the mass has been calculated (as given in col. [10]) or, in cases where this radius is unavailable, the nominal King limiting radius (denoted r_{lim}). Col. (5): Mass within the radius in col. (4) based on modeling of extended dispersion profile. Col. (6): Mean density within the radius in col. (4). Col. (7): Mean density within 10 pc assuming mass is distributed as a power law with $\rho \propto r^{-1}$. Col. (8): Circular speed at edge of data $=(GM_{dark}/r)^{1/2}$. Col. (9): Estimated mean phase-space density within half-light radius $=3/(8\pi G r_h^2 \sigma)$. See text for an explanation. Col. (10): Reference.

REFERENCES.—(1) Walker et al. 2006; (2) Koch et al. 2007b; (3) Mateo 1998; Westfall et al. 2006; (4) Coleman et al. 2007; Koch et al. 2007a; (5) Kleyna et al. 2004; Wilkinson et al. 2006; (6) Wilkinson et al. 2006; (7) Wilkinson et al. 2004; (8) Belokurov et al. 2006b; Muñoz et al. 2006a; (9) Willman et al. 2005a; Kleyna et al. 2005.

cases where additional information is available cored density profiles are preferred.

In Table 3 we summarize the mass determination results available. The most robust numbers are the cumulative mass within the extent of the kinematic data, and the associated mean density and outer circular speed (Table 3, cols. [5], [6], and [8]). The central density is more model dependent. As an illustration of the range of likely values, column (7) gives the mean density within 10 pc in the case in which the dark matter has a density profile which goes as $\rho \propto r^{-1}$ throughout the volume occupied by the stellar distribution. If the dark matter has approximately constant density out to some break radius, as our models prefer, then its central density will, of course, be comparable to the mean density quoted in column (6). Table 3 also provides an estimate of the mean phase-space density within the half-light radius, which is defined as $3/(8\pi G r_h^2 \sigma)$. This estimate assumes that the half-mass radius is comparable to the observed half-light radius and that the stellar velocity dispersion is related to the total mass through $\sigma^2 = GM/r_h$. Since neither assumption is strictly valid (cols. [3] and [5] show that this yields an underestimate of the true mass) column (9) should be interpreted as an order-of-magnitude estimate only.

The total masses within the optical radii of the dSph galaxies have been suspected for some years of showing a remarkably small range. Mateo (1998) showed that the available data at the time were consistent with an apparent minimum dark halo mass, within the optical galaxy, of the order of $10^7\ M_\odot$. This relationship was extended and developed by Côté et al. (1999), who showed it also applied to available data from M31 satellites. Later updates were provided by Wilkinson et al. (2006) and by Gilmore et al. (2007). The current version of that relationship is shown in Figure 5. Remarkably, the Mateo proposal has survived an increase in the dynamic range of the sample by an order of magnitude in both axes and has become better established, and of lower scatter, as newer data have become available.

The Mateo plot presents total dark masses within the optical radii. A total mass is the integral over a scale length, a mass density profile, and a central mass-density normalization. Each of those parameters is addressed in this paper. The photometric scale lengths are summarized in Figure 1, which illustrates that dSph galaxies have both a minimum scale size (~120 pc) and a rather small range of scale sizes. The available kinematic data and their analyses are discussed above, summarized in Figure 4. That shows that each galaxy studied, under the assumption of a valid Jeans equation analysis, has a similar mass profile, both in shape and in normalization: in at least two cases it is probably cored, and the central density, assuming a cored profile, is then very similar for all cases analyzed to date. For clarity, we note that we have no robust independent proof that the photometric scale length is exactly the underlying mass scale length. From the mass

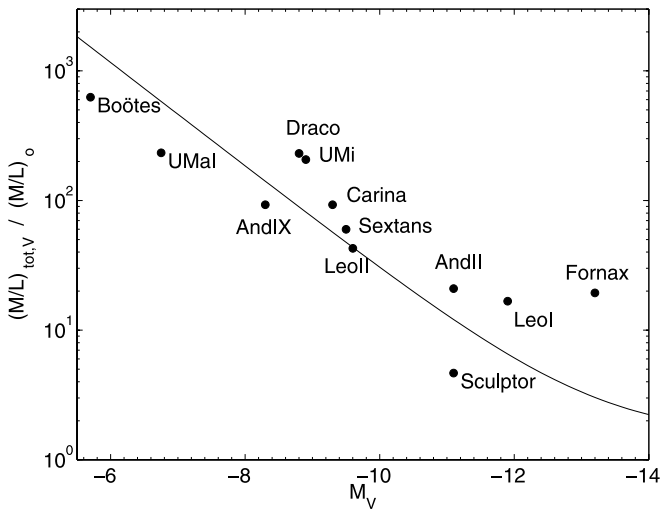

FIG. 5.—Updated Mateo plot. Mass-to-light ratios are plotted vs. absolute magnitudes for Local Group dwarf galaxies, following a style suggested by Mateo et al. (1993) and Mateo (1998, his Fig. 9, *bottom panel*). The solid line is the relation for a constant mass (dark) halo. The modern data shown here extend the original relation by three magnitudes in luminosity and an order of magnitude in mass-to-light ratio, while reducing the scatter by an order of magnitude. Data are from the tables in the text, except for And II (Côté et al. 1999) and And IX (Chapman et al. 2005). Values for Sculptor, And II, And IX, UMa I, and Bootes are based on small kinematic samples and are less certain than are the results for the other galaxies. We explain this correlation as a consequence of the characteristic minimum galaxy scale size shown in Fig. 1 convolved with the narrow range of mass profiles and mean dark matter densities shown in Fig. 4.

modeling, the lower limit on mass density core size is constrained to be at most a factor of 2 smaller than the observed luminosity core in UMi and Fornax. Similarity, rather than exact equality, of the two scales is what we are assuming here. Constancy of the scale length, the normalization, and the density profile parameters naturally explains the Mateo plot, which is their product.

3.7. *Are These Derived Properties Robust?*

The photometric (length scale) data are described above, and shown to be robust for star clusters and conservative relative to the present conclusions for galaxies.

There are two dynamical effects of relevance to bear in mind. In dense star clusters the very steep and highly time-dependent gravitational potential gradient between binary stars (especially close binaries) provides a force which could eject dark matter particles. Essentially, close binary stars will orbit through the cluster threshing the local potential gradient, clearing a dynamical tunnel through phase space and ejecting any dark matter particles which might have been present. Such an effect will be particularly important in the central regions of star clusters, which are continually occupied by close binaries. This effect is worth additional consideration and suggests that more extensive numerical modeling and kinematic studies of the outer parts of diffuse star clusters is worthwhile. Significant dynamical evolution will be irrelevant in systems whose internal dynamical relaxation time is much longer than its age. We show above that all the small galaxies of interest here in fact will be immune to this effect.

The second important consideration concerns the validity of the assumed steady state dynamical analysis. There is continuing debate and study of the possible relevance of time dependence in dynamical analyses of dSph galaxy stellar kinematics. Time-dependent tidal disruption is manifestly dominant in the most nearby dSph galaxy, Sagittarius, and is probably relevant for other dSph galaxies within a few tens of kiloparsecs from the Galactic center (Coma Berenices and UMa II are the obvious candidates). In the more distant galaxies there is no kinematic evidence that the internal stellar kinematics in their central regions are in any way affected by external Galactic tides (Koch et al. 2007b). Most—but not all—kinematic studies remain limited to moderate sample sizes, so that necessarily statistical and model-dependent removal of interlopers and outliers can affect conclusions somewhat (e.g., Klimentowski et al. 2007). Similar conclusions have very recently been derived by Wu (2007) in his parametric reanalysis of published data for Draco, Fornax, and UMi. Wu concludes: "Because [his distribution function] models can fit both radial velocity profiles and surface number density profiles, the so-called extra-tidal extensions in the surface number density profiles found by Irwin & Hatzidimitriou (1995) and Wilkinson et al. (2004) do not require any special ad hoc explanation. Thus it is not valid to consider them as the evidence of tidal stripping, as proposed by some authors (e.g., Martínez-Delgado et al. 2001; Gómez-Flechoso & Martínez-Delgado 2003; Muñoz et al. 2005)."

We note for completeness that there are continuing efforts to apply pure tidal models—i.e., there is no dark matter, and the velocity dispersions are inflated by tides—to dSph kinematics. If these models can be proven to be relevant, the implications for the nature of dark matter are quite profound. Substantially longer minimum length scales and substantially lower maximum mass densities even than those derived here will be required, providing quite extreme constraints on the nature of dark matter. It remains far from clear that such mass-follows-light models are consistent with the robust evidence on cosmological scales that dark matter dominates the universe.

4. DISCUSSION AND IMPLICATIONS

There is strong, and strengthening, observational evidence for four conclusions concerning the smallest galaxies and typical or brighter (globular, nuclear) star clusters. These two families of objects coexist over the range of stellar absolute magnitudes from $-15 \lesssim M_V \lesssim -4$, corresponding to luminosities from $\sim 10^9\ L_\odot \gtrsim L \gtrsim 10^3\ L_\odot$, with the upper limit corresponding to the brightest known star clusters (Seth et al. 2006; Hilker et al. 2007; Evstigneeva et al. 2007), the lower limit to the least luminous galaxies yet discovered (Belokurov et al. 2007). The number of well-studied objects known within these limits in both classes has increased substantially in recent years, providing an adequate sample to identify systematics and to test earlier, provisional trends (Côté et al. 1999; Wilkinson et al. 2006).

We conclude the following.

1. Over this substantial dynamic range, there is a clear bimodality in the size distributions of the two families of object: all smaller objects are star clusters and have characteristic scale sizes $\lesssim$30 pc ($\lesssim 10^{18}$ m), while all larger objects are galaxies and have scale sizes for their luminous (stellar) components $\gtrsim$120 pc ($\gtrsim 4 \times 10^{18}$ m).

2. Where kinematic studies exist (essentially in the central luminous regions), there is a clear distinction between the phase-space distribution functions of star clusters and galaxies. At a given (stellar, baryonic) luminosity, galaxies have phase-space densities typically 2–3 orders of magnitude lower than do star clusters. In all adequately studied cases, the galaxy's luminous stellar component is embedded in a more extended dark matter halo. Star clusters over the whole mass range are well described by the virial theorem and show no evidence for any (dynamically significant, extended) dark matter halos.

3. In the two specific galaxies where both detailed dynamical analyses are feasible, i.e., substantial kinematic data across the face of the galaxies are available, and where independent evidence to break the core/cusp/velocity-anisotropy mass degeneracy exists, the derived dark mass distribution has a shallow density profile. For a density distribution ρ describable as a function of radius r as $\rho(r) \propto r^{-\alpha}$, the data imply that the power-law index $\alpha \lesssim 0.5$, where α is consistent with zero in the innermost regions. Simplicity argues for this being the general case. Under that assumption of generality, the minimum photometric length scale can be interpreted as comparable to a minimum length scale for the clustering of dark matter. The lower limit on the size of a mass density core is constrained to be at most a factor of 2 smaller than the observed luminosity scale, while our dynamical modeling suggests it is not much, if at all, larger.

4. Using the mass model assumed in point 3, the derived mean mass density of dark matter within one to two half-light radii for all the galaxies is $\rho_{\rm DM} \lesssim 5\ {\rm GeV}/c^2\ {\rm cm}^{-3}$ (about $0.1\ M_\odot\ {\rm pc}^{-3}$). If we do not adopt the results of point 3 but allow a cusped mass model, the derived maximum mass density of dark matter within 10 pc of the center is $\rho_{\rm max,DM} \lesssim 2\ {\rm TeV}/c^2\ {\rm cm}^{-3}$ (about $60\ M_\odot\ {\rm pc}^{-3}$).

The combination of the small range of observed scale sizes, together with an apparently standard (isochrone-like) form for the derived dark mass density profile and its normalization, naturally explains the observed relation that all dSph galaxies have similar total dark mass within their optical radii.

These systematic properties have obvious implications for the nature of dark matter and galaxy formation in small halos, which we note very briefly here. The simplest case is that our cored mass profiles are the unmodified outcome of formation of

small halos. An alternative is that dark matter profiles on these small scales have been drastically restructured by some astrophysical (feedback) process. We very briefly note each in turn.

4.1. *Implications for ΛCDM Galaxy Formation Models*

One immediately asks if our observed length scale and characteristic upper mass density derived here for the intrinsic nature of dark matter is consistent with the extremely high quality agreement between ΛCDM models and large-scale structure, assuming the shallow small-scale profiles are an intrinsic feature of dark matter halo formation. Few (if any) cosmological observations of large-scale structure have resolution on small enough scales to be sensitive to the truncation of the small-scale power spectrum on scales of the order of 100 pc implied here, so there is no disagreement. Galaxy formation models inside the ΛCDM paradigm, however, have considerable difficulties matching observations on small scales. The well-known "satellite problem" is an example, as is the "cores versus cusps" debate. The amount of structure on subkiloparsec scales predicted by simulations will be very drastically modified by our conclusions here, which imply that the primordial power spectrum is truncated at small physical length scales. In both the satellite counts and the core-cusp debates, the discordance between data and numerical models will be greatly reduced in simulations which include the minimum scale cutoff suggested by our results. Numerical studies are underway to quantify this.

A fundamental astrophysical, rather than dark matter, puzzle which is not simply explained is the now well-established bimodal size distribution function illustrated in our Figure 1. Star clusters have a maximum half-light scale size of some 30 pc, while the characteristic minimum scale length associated with the stellar systems which occupy dark matter halos is some 4–5 times larger. The dark matter mass profiles derived here have a scale length always a factor of several longer than the scale on which self-gravitating star clusters form. But why do stellar systems not form with all possible scale lengths inside the shallow dark matter potentials which we observe kinematically? It is a generic prediction of ΛCDM galaxy formation models that the baryonic component should cool and collapse by a factor of $\lambda^{-1} \approx 10$ more than does the (presumed self-interaction free) dark matter. Why is this not seen in these very low mass halos?

It seems that stellar populations in these shallow potentials expand to a scale size comparable to that of the underlying potential. An attempted explanation is beyond our present purposes. We note, however, that there are many studies of feedback in shallow potential wells (see, e.g., Dekel & Silk 1986; Silk et al. 1987; Read et al. 2006a; Mayer et al. 2007) which discuss the clear importance of energy balance in driving gas loss and in expanding extant stellar systems. We have attempted an explanation of this ourselves (Read & Gilmore 2005), concluding that plausible astrophysical feedback capable of leaving a dSph-like remnant cannot convert a cusped DM profile into a cored DM profile, but extended shallow (exponential) dSph luminosity can be readily formed. More generally Read et al. (2006a) provide an extensive discussion and introduction to the literature. Several of these models remove all residual gas in an early star formation episode, with the lost gas-mass reducing the binding energy of the residual stellar system, allowing it to expand into the dark matter potential. A further general constraint on these promising models is that many dSph galaxies have supported extended star formation, and some show evidence for internal chemical element self-enrichment, sometimes over most of the age of the universe. Derived star formation rates tend to be very low—of the order of one star per 10^5 yr—so that single disruptive gas-evacuation events are not part of solution space (e.g., Hernandez et al. 2000; Carigi et al. 2002). Such disruptive events are of course consistent with the apparent absence of stellar systems occupying dark halos of lower mass than those we observe, should they be more prevalent on smaller mass scales than we study here.

4.2. *Implications for the Nature of Dark Matter*

An adequate discussion is beyond our intention in this paper, which is to establish the observational evidence. The local dark matter mass density near the Sun was determined using distribution function modeling to have the value $\rho_{\rm DM} \sim 0.3$ GeV/c^2 cm^{-3} (about 0.01 $M_\odot$ pc^{-3}; Kuijken & Gilmore 1989, 1991). Our maximum mass density and minimum physical length scale derived here imply particle number densities and self-interaction cross sections (if one assumes self-interaction is the physical cause of the present-day length scale), which are readily calculable for any specific particle class. We note only the obvious conclusion that the very low maximum mass density derived here is challenging for models of dark matter which are dominated by massive (of order TeV) particles, such as those predicted by some supersymmetric theories. Such particles would be required to have a spatial number density $\lesssim$1 cm^{-3} even if the mass density profile is cusped and orders of magnitude lower if our cored profiles are appropriate. Much lower mass (μeV) particles, such as the axion, would have correspondingly higher number densities. Rather interestingly, intermediate-mass (keV) sterile neutrino particles have been discussed (see, e.g., Dodelson & Widrow 1994; Abazajian et al. 2001; Kusenko 2006; Biermann & Munyaneza 2007a, 2007b) as relevant in just the spatial and density range we have derived here.

A. K. and E. K. G. acknowledge support by the Swiss National Science Foundation through grant 200020-105260.

REFERENCES

Abazajian, K., Fuller, G. M., & Patel, M. 2001, Phys. Rev. D, 64, 023501
An, J. H., & Evans, N. W. 2006, ApJ, 642, 752
Bastian, N., Saglia, R. P., Goudfrooij, P., Kissler-Patig, M., Maraston, C., Schweizer, F., & Zoccali, M. 2006, A&A, 448, 881
Battaglia, G., et al. 2006, A&A, 459, 423
Belokurov, V., et al. 2006a, ApJ, 642, L137
———. 2006b, ApJ, 647, L111
———. 2007, ApJ, 654, 897
Bender, R., Burstein, D., & Faber, S. 1992, ApJ, 399, 462
Biermann, P. L., & Munyaneza, F. 2007a, preprint (astro-ph/0702164)
———. 2007b, preprint (astro-ph/0702173)
Binney, J., & Tremaine, S. 1987, Galactic Dynamics (Princeton: Princeton Univ. Press)
Brodie, J. P., & Larsen, S. 2002, AJ, 124, 1410
Burstein, D., Bender, R., Faber, S., & Nolthenius, R. 1997, AJ, 114, 1365
Carigi, L., Hernandez, X., & Gilmore, G. 2002, MNRAS, 334, 117
Chapman, S. C., Ibata, R., Lewis, G. F., Ferguson, A. M. N., Irwin, M., McConnachie, A., & Tanvir, N. 2005, ApJ, 632, L87
Coleman, M. G., Jordi, K., Rix, H.-W., Grebel, E. K., & Koch, A. 2007, AJ, submitted
Côté, P., Mateo, M., Olszewski, E., & Cook, K. 1999, ApJ, 526, 147
Dekel, A., & Silk, J. 1986, ApJ, 303, 39
De Propris, R., Phillipps, S., Drinkwater, M. J., Gregg, M. D., Jones, J. B., Evstigneeva, E., & Bekki, K. 2005, ApJ, 623, L105
Dodelson, S., & Widrow, L. 1994, Phys. Rev. Lett., 72, 17
Drinkwater, M. J., Gregg, M. D., Hilker, M., Bekki, K., Couch, W. J., Ferguson, H. C., Jones, J. B., & Phillipps, S. 2003, Nature, 423, 519
Evstigneeva, E. A., Gregg, M. D., Drinkwater, M. J., & Hilker, M. 2007, AJ, 133, 1722
Fall, S. M., & Rees, M. J. 1977, MNRAS, 181, P37

Fellhauer, M., et al. 2007, MNRAS, 375, 1171
Gilmore, G., Wilkinson, M., Kleyna, J., Koch, A., Evans, N. W., Wyse, R. F. G., & Grebel, E. K. 2007, Nucl. Phys. B, in press (astro-ph/0608528)
Gnedin, O., & Ostriker, J. P. 1997, ApJ, 474, 223
Goerdt, T., Moore, B., Read, J. I., Stadel, J., & Zemp, M. 2006, MNRAS, 368, 1073
Gómez, M., Geisler, D., Harris, W. E., Richtler, T., Harris, G. L. H., & Woodley, K. A. 2006, A&A, 447, 877
Gómez-Flechoso, M. Á., & Martínez-Delgado, D. 2003, ApJ, 586, L123
Green, A. A., Hofman, S., & Schwarz, D. J. 2005, in AIP Conf. Proc. 805, 11th International Symposium on Particles, Strings and Cosmology, ed. K. Choi, J. E. Kim, & D. Son (Melville: AIP), 431
Grillmair, C. J. 2006, ApJ, 645, L37
Harbeck, D., et al. 2001, AJ, 122, 3092
Harris, W. E. 1996, AJ, 112, 1487
Harris, W. E., Harris, G. L. H., Barmby, P., McLaughlin, D. E., & Forbes, D. A. 2006, AJ, 132, 2187
Harris, W. E., Harris, G. L. H., Holland, S. T., & McLaughlin, D. E. 2002, AJ, 124, 1435
Haşegan, M., et al. 2005, ApJ, 627, 203
Hernandez, X., Gilmore, G., & Valls-Gabaud, D. 2000, MNRAS, 317, 831
Hilker, M. 2006, A&A, 448, 171
Hilker, M., Baumgardt, H., Infante, L., Drinkwater, M., Evstigneeva, E., & Gregg, M. 2007, A&A, 463, 119
Ibata, R., Chapman, S., Irwin, M., Lewis, G., & Martin, N. 2006, MNRAS, 373, L70
Irwin, M., & Hatzidimitriou, D. 1995, MNRAS, 277, 1354
Johnston, K., Choi, P. I., & Guharthakurta, P. 2002, AJ, 124, 127
Johnston, K., Sigurdsson, S., & Hernquist, L. 1999, MNRAS, 302, 771
King, I. 1966, AJ, 71, 64
Klessen, R. S., Grebel, E. K., & Harbeck, D. 2003, ApJ, 589, 798
Kleyna, J. T., Wilkinson, M. I., Evans, N. W., & Gilmore, G. 2001, ApJ, 563, L115
———. 2004, MNRAS, 354, L66
———. 2005, ApJ, 630, L141
Kleyna, J., Wilkinson, M. I., Evans, N. W., Gilmore, G., & Frayn, C. 2002, MNRAS, 330, 792
Kleyna, J. T., Wilkinson, M. I., Gilmore, G., & Evans, N. W. 2003, ApJ, 588, L21
Klimentowski, J., Lokas, E. L., Kazantzidis, S., Prada, F., Mayer, L., & Mamon, G. A. 2007, MNRAS, 378, 353
Klypin, A., Kravtsov, A. V., Valenzuela, O., & Prada, F. 1999, ApJ, 522, 82
Koch, A., Grebel, E. K., Kleyna, J. T., Wilkinson, M. I., Harbeck, D. R., Gilmore, G. F., Wyse, R. F. G., & Evans, N. W. 2007a, AJ, 133, 270
Koch, A., Wilkinson, M. I., Kleyna, J. T., Gilmore, G. F., Grebel, E. K., Mackey, A. D., Evans, N. W., & Wyse, R. F. G. 2007b, ApJ, 657, 241
Kormendy, J. 1985, ApJ, 295, 73
Kormendy, J., & Freeman, K. C. 2004, in IAU Symp. 220, Dark Matter in Galaxies, ed. S. D. Ryder et al. (San Francisco: ASP), 377
Kuijken, K., & Gilmore, G. 1989, MNRAS, 239, 605
———. 1991, ApJ, 367, L9
Kusenko, A. 2006, preprint (hep-ph/0609158)
Lokas, E. L. 2002, MNRAS, 333, 697
Lokas, E. L., Mamon, G. A., & Prada, F. 2005, MNRAS, 363, 918
Mackey, A. D., et al. 2006, ApJ, 653, L105
Magorrian, J. 2003, in The Mass of Galaxies at Low and High Redshift, ed. R. Bender & A. Renzini (Berlin: Springer), 18
Martin, N. F., Ibata, R. A., Irwin, M. J., Chapman, S., Lewis, G. F., Ferguson, A. M. N., Tanvir, N., & McConnachie, A. W. 2006, MNRAS, 371, 1983
Martínez-Delgado, D., Alonso-García, J., Aparicio, A., & Gómez-Flechoso, M. A. 2001, ApJ, 549, L63
Mateo, M. 1997, in ASP Conf. Ser. 116, The Nature of Elliptical Galaxies, ed. M. Arnaboldi, G. S. Da Costa, & P. Saha (San Francisco: ASP), 259
Mateo, M. L. 1998, ARA&A, 36, 435
Mateo, M., Olszewski, E. W., Pryor, C., Welch, D. L., & Fischer, P. 1993, AJ, 105, 510
Mayer, L., Katzantzidis, S., Mastropietro, C., & Wadsley, J. 2007, Nature, 445, 738
McConnachie, A. W., Peñarrubia, J., & Navarro, J. F. 2006, ApJ, submitted (astro-ph/0608687)
Mieske, S., Hilker, M., & Infante, L. 2002, A&A, 383, 823
Moore, B., Ghigna, S., Governato, F., Lake, G., Quinn, T., Stadel, J., & Tozzi, P. 1999, ApJ, 524, L19
Muñoz, R. R., Carlin, J. L., Frinchaboy, P. M., Nidever, D. L., Majewski, S. R., & Patterson, R. J. 2006a, ApJ, 650, L51
Muñoz, R. R., et al. 2005, ApJ, 631, L137
———. 2006b, ApJ, 649, 201
Navarro, J., Frenk, C., & White, S. D. M. 1997, ApJ, 490, 493
Odenkirchen, M., et al. 2001, AJ, 122, 2538
———. 2003, AJ, 126, 2385
Ostriker, J. P., & Steinhardt, P. 2003, Science, 300, 1909
Penarrubia, J., McConnachie, A., & Navarro, J. 2007, ApJ, submitted (astro-ph/0701780)
Read, J. I., & Gilmore, G. 2005, MNRAS, 356, 107
Read, J. I., Pontzen, A. P., & Viel, M. 2006a, MNRAS, 371, 885
Read, J. I., Wilkinson, M. I., Evans, N. W., Gilmore, G., & Kleyna, J. T. 2006b, MNRAS, 367, 387
Ségall, M., Ibata, R. A., Irwin, M. J., Martin, N. F., & Chapman, S. 2007, MNRAS, 375, 831
Seitzer, P. O. 1983, Ph.D. thesis, Univ. Virginia
Seth, A. C., Dalcanton, J. J., Hodge, P. W., & Debattista, V. P. 2006, AJ, 132, 2539
Silk, J., Wyse, R. F. G., & Shields, G. 1987, ApJ, 322, L59
Sohn, S. T., et al. 2007, ApJ, in press (astro-ph/0608151)
Tolstoy, E., et al. 2004, ApJ, 617, L119
Walcher, C. J., et al. 2005, ApJ, 618, 237
Walker, M. G., Mateo, M., Olszewski, E. W., Bernstein, R., Wang, X., & Woodroofe, M. 2006, AJ, 131, 2114
Westfall, K. B., Majewski, S. R., Ostheimer, J. C., Frinchaboy, P. M., Kunkel, W. E., Patterson, R. J., & Link, R. 2006, AJ, 131, 375
Wilkinson, M. I., Kleyna, J. T., Evans, N. W., & Gilmore, G. 2002, MNRAS, 330, 778
Wilkinson, M. I., Kleyna, J. T., Evans, N. W., Gilmore, G., Irwin, M., & Grebel, E. K. 2004, ApJ, 611, L21
Wilkinson, M. I., Kleyna, J. T., Evans, N. W., Gilmore, G. F., Read, J. I., Koch, A., Grebel, E. K., & Irwin, M. J. 2006, EAS Publ. Ser., 20, 105
Willman, B., et al. 2005a, ApJ, 626, L85
———. 2005b, AJ, 129, 2692
———. 2006, AJ, submitted (astro-ph/0603486)
Wu, X. 2007, ApJ, submitted (astro-ph/0702233)
Wyse, R. F. G., Gilmore, G., Houdashelt, M. L., Feltzing, S., Hebb, L., Gallagher, J. S., & Smecker-Hane, T. A. 2002, NewA, 7, 395
Zaritsky, D., Gonzalez, A. H., & Zabludoff, A. I. 2006a, ApJ, 638, 725
———. 2006b, ApJ, 642, L37
Zucker, D. B., et al. 2004, ApJ, 612, L121
———. 2006a, ApJ, 643, L103
———. 2006b, ApJ, 650, L41
———. 2007, ApJ, 659, L21